Time-Integrated Bioavailability Proxy for Actinides in a Contaminated Estuary

Joshua D. Chaplin,* Marcus Christl, Andrew B. Cundy, Phillip E. Warwick, Paweł Gaca, François Bochud, and Pascal Froidevaux*

Cite This: *ACS EST Water* 2022, 2, 1688−1696

Read Online

ACCESS | ~~Metrics & More~~ | ~~Article Recommendations~~

ABSTRACT: Actinides accumulate within aquatic biota in concentrations several orders of magnitude higher than in the seawater [the concentration factor (CF)], presenting an elevated radiological and biotoxicological risk to human consumers. CFs currently vary widely for the same radionuclide and species, which limits the accuracy of the modeled radiation dose to the public through seafood consumption. We propose that CFs will show less dispersion if calculated using a time-integrated measure of the labile (bioavailable) fraction instead of a specific spot sample of bulk water. Herein, we assess recently developed configurations of the diffusive gradients in thin films (DGT) sampling technique to provide a more accurate predictor for the bioaccumulation of uranium, plutonium, and americium within the biota of the

Sellafield-impacted Esk Estuary (UK). We complement DGT data with the cross-flow ultrafiltration of bulk seawater to assess the DGT-labile fraction versus the bulk concentration. Sequential elution of *Fucus vesiculosis* reveals preferential internalization and strong intracellular binding of less particle-reactive uranium. We find significant variations between CF values in biota calculated using a spot sample versus using DGT, which suggest an underestimation of the CF by spot sampling in some cases. We therefore recommend a revision of CF values using time-integrated bioavailability proxies.

KEYWORDS: *plutonium, uranium, americium, diffusive gradients in thin films/DGT, bioaccumulation, concentration factor, radiation dose modeling, sellafield*
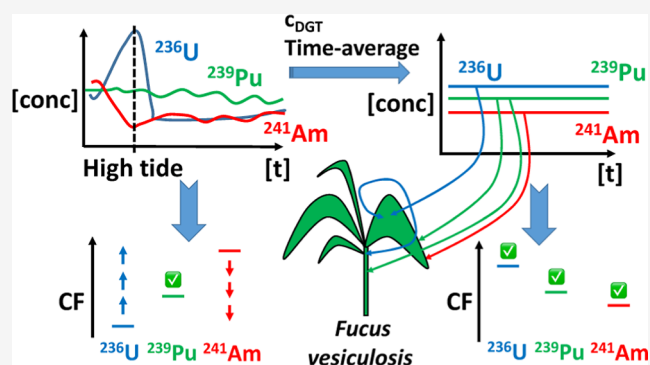
INTRODUCTION

Actinides are widely dispersed in the environment from a range of anthropogenic nuclear discharges. Isotopes of plutonium, americium, and uranium are among the most radiologically significant radionuclides in the oceans due to their long half-lives, alpha-particle emissions, and significant inventories in seawater and sediments. Despite their dilution in seawater, accumulations of these actinides within aquatic organisms can be several orders of magnitude higher than their waterborne concentration[1−9] [their concentration factor (CF)]. The accumulation of actinides within marine biota must therefore be monitored to ensure that the radiation dose received by human consumers does not reach hazardous levels. This is especially pertinent at sites where nuclear discharges have supplied the local waters and sediments with a significant supply of radionuclides such as the Cumbrian coastal environment, which is labelled with historic radionuclide discharges from the UK's Sellafield facility.[6,10−14]

Understanding the controls on actinide bioavailability includes determining the speciation of the radionuclide in the water. This is dependen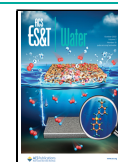t on fluctuating site-specific physicochemical conditions which affect the behavior of the radionuclide, including its association with colloids and suspended particulate matter (SPM), dictating its environmental mobility and the lability of the complexes it forms. CFs have been widely used to describe the transfer of radionuclides from water, including seawater, to organisms.[1−9] CFs allow a rapid but unspecific evaluation of the radionuclide activity in an organism (*e.g.*, species of fish and shellfish) based on dividing the concentration of a radionuclide in the organism per unit wet mass (c_{org}) by the bulk water concentration (c_{bulk}). However, c_{bulk} is not an unfailing indicator for predicting the radiological risks of a radionuclide; CFs suffer a very large dispersion of values for the same radionuclide and species between numerous studies[1−9] and are noted by the Interna-

tional Atomic Energy Agency (IAEA) to have limitations due to environmental physicochemical variations.[15] In this respect, c_{bulk} could be replaced with a more representative time-weighted average concentration which accounts for fluctuating hydrological chemistry, especially in areas with a dynamic hydraulic regime which significantly affects the waterborne metal concentrations, such as estuaries. Furthermore, exclusively measuring the bioavailable fraction of a radionuclide (that which can be taken up by biota) may provide more accuracy for the calculation of a CF. To predict the radiological risk to the biota, a reliable *in situ* approach is therefore required to representatively assess the time-averaged concentration and bioavailability of a radionuclide. The development of simple methods to determine the bioavailability of a specific radioelement is therefore a prerequisite to gather data that can be used in studies of dose risk assessment to the public.

The diffusive gradients in thin films (DGT) sampling technique provides an *in situ* time-weighted average concentration of free and labile species which are fully bioavailable to organisms (c_{DGT}, eq 4 of methods).[16] We therefore propose that c_{DGT} should provide a more valid measure of the waterborne concentration than c_{bulk}, as it takes into account fluctuating site-specific geochemical characteristics which affect metal-complex lability. Furthermore, diffusion through the DGT sampler's material diffusion layer mimics the passive uptake of trace labile elements by organisms through their cell membrane. In this respect, we propose that c_{DGT} gives a more realistic estimate of the bioavailable fraction of actinides in sea water than c_{bulk} and consequently that CFs for a given radionuclide and species will show less dispersion by calculating using c_{org}/c_{DGT} rather than c_{org}/c_{bulk}.

In this work, we deployed recently developed DGT configurations for measures of U, Pu, and Am[17,18] (collectively "the target actinides") in middle and lower estuary environments within the Esk Estuary (UK), which is a subcomponent of the macrotidal Ravenglass Estuary system. The Esk Estuary has been impacted by historic radionuclide discharges from the nearby Sellafield facility and has a highly dynamic hydraulic regime, which is known to significantly affect metal concentrations in the water throughout the tidal cycle.[19] We complemented DGT data with cross-flow ultrafiltration (CFUF) work on spot-sampled seawater to determine the SPM-associated and colloid-associated fractions of the target actinides and sequential elution (SE) of common seaweed [*Fucus vesiculosis* (*F. vesiculosis*)] to determine the internal distribution of the target actinides. Working with U, Pu, and Am allowed us to assess the geochemical behavior of three radioelements with significantly different degrees of particle reactivity. Samples were measured by ultrasensitive accelerator mass spectrometry (AMS) using the actinide-optimized TANDY AMS facility at ETH Zürich.[20] AMS enabled subfemtogram masses of some isotopes in the DGT gel eluates to be determined, including the low-abundance anthropogenic isotope ^{236}U.

■ MATERIALS AND METHODS

Materials. All reagents used to manufacture DGT resin-gels and to radiochemically process samples were of analytical grade. The KMS-1 resin was synthesized as reported by Manos *et al.*[21] The IIP-Y^{3+} resin was synthesized in a modified procedure following that reported by Chauvin *et al.*[22] but using the modified ligand L_1 synthesis reported by Chaplin *et al.*[17] KMS-1 and IIP-Y^{3+} resin-gels were synthesized according to

the procedures reported by Chaplin *et al.*[17] Diffusive gels and filter membranes were purchased from DGT Research (Lancaster, UK). DGT configurations for seawater deployments were assembled within custom 105 cm^2-surface area DGT samplers as reported by Cusnir *et al.*[23] 1−5 pg each of ^{232}U, ^{242}Pu, and ^{243}Am ("the tracers") were added to samples prior to radiochemical separations at the stages described during sample treatment in the following sections.

Site Selection and Sampling. Samples were collected at two sites in the middle and lower Esk Estuary, with the lower estuary site closest to estuary mouth and exit to the Irish sea (Figure 1). At each site, KMS-1 and IIP-Y^{3+} DGT

Figure 1. Middle and lower estuary sampling sites (red circles), Esk Estuary, Cumbria, UK with the Sellafield nuclear site situated 10 km north (marked).

configurations within 105 cm^2-surface area DGT samplers were deployed for 14 days between 24 May and 7 June 2021. Two samplers of each configuration, assembled with different diffusive gel thicknesses of 0.39 and 0.78 mm, were deployed within stainless-steel housings and secured to fixed objects in the substrate at around a 45° upright angle tangential to the current. No evidence of significant biofouling or sedimentation on the filter membranes was observed when retrieving the samplers. 25 L of seawater samples and samples of *F. vesiculosis* were obtained adjacent to the sites of DGT sampler deployment at both the lower and middle estuary sites.

CFUF. 25 L of seawater samples were passed through 0.45 μm filters. The filters were desiccated and calcinated for analysis. U, Pu, and Am were eluted from the ashed filters by leaching overnight in 8 M HNO$_3$. The eluate was spiked with the tracers, filtered through a 0.45 μm syringe filter, and prepared for radiochemical separations. U, Pu, and Am in this fraction were attributed to the SPM-associated fraction. An aliquot of the filtered seawater was kept for measure as the bulk fraction. A separate aliquot was subject to CFUF using a 1 ft^2 10 kDa Millipore Prep/Scale-TFF membrane until a CF between the retentate and permeate fractions (cf_{UF}) of >7 was reached, according to eq 1.

$$cf_{UF} = \frac{v_{perm}}{v_{ret}} \tag{1}$$

Here, v_{perm} is the volume (L) of the permeate fraction and v_{ret} is the volume (L) of the retentate fraction. The bulk, permeate, and retentate fractions were spiked with the tracers, and 0.25 g of FeCl$_3$·6H$_2$O per 10 L of sample was added while mixing at 500 rpm and heating at 80 °C. After at least 30 min of equilibration, U, Pu, and Am were coprecipitated with Fe at pH > 7 by dropwise addition of NH$_4$OH (30%) and prepared for radiochemical separations.

SE of actinides from Seaweed. To investigate the internal distribution of the target actinides within *F. vesiculosis* retrieved at each sampling site, we used SE to distinguish (a) the fraction of each actinide externally coprecipitated onto the fronds, (b) the fraction accumulated extracellularly as cations bound to exchange sites on the cell wall and plasma membrane, (c) the fraction accumulated intracellularly in a still-soluble form which can be washed out of the cytosol, and (d) the fraction strongly bound intracellularly to the particulate plant material or incorporated into polymeric molecules (*e.g.*, proteins and lipids). These fractions were compared with c_{DGT} and c_{bulk} between the lower and middle estuary sites to assess the controls of actinide speciation on accumulation and distribution in *F. vesiculosis*. SE was performed on *F. vesiculosis* samples, following the method described by Vázquez *et al.*[24] for heavy metal SE from bryophytes. Bulk *F. vesiculosis* samples were washed with deionized water to remove the sediment. *F. vesiculosis* was then immersed in a citrate buffer (1 L 0.1 M citric acid/0.1 M sodium citrate) for 1 h. This step dissolved the actinides which were externally coprecipitated on the plants, most likely with carbonate[25] (the "external" fraction). *F. vesiculosis* was removed after an hour and rinsed with deionized water, with the washout added to the external fraction. *F. vesiculosis* was then immersed in 1 L of 10 mM ethylenediaminetetraacetic acid (EDTA) for 1 h to displace actinide cations bound to ion-exchange sites on the cell wall and plasma membrane (the "extracellular" fraction). *F. vesiculosis* was removed from the EDTA after an hour and rinsed with deionized water, with the washout added to the extracellular fraction. *F. vesiculosis* was then desiccated at 80 °C for 24 h to destroy the cell walls of the plants and subsequently immersed in 1 M HNO_3 for 1 h to leach soluble actinides from within the cells (the "intracellular" fraction). *F. vesiculosis* was removed from 1 M HNO_3 and thoroughly rinsed with deionized water as before. The external, extracellular, and intracellular fractions were filtered through a 0.45 μm membrane using a Büchner filter. The remaining *F. vesiculosis* (the "residual" fraction) was redesiccated for 24 h before calcination at 550 °C overnight. The ashes and 20 mL of concentrated HNO_3 and the tracers were added to Teflon canisters, before wet ashing in a microwave reactor at 180 °C under 50 bars pressure (Milestone UltraClave IV, Germany). The tracers were added to each of the four *F. vesiculosis* fractions. An aliquot of each fraction was precipitated with calcium oxalate to prepare it for the measurement of Pu and Am. The oxalate precipitate was decanted, centrifuged, and reacidified in 20 mL of concentrated HNO_3. 6 mL of H_2O_2 was then added, and the oxalate was destroyed in the microwave reactor at 180 °C under 50 bars pressure. A separate aliquot of each of the four *F. vesiculosis* fractions was prepared for the measure of U by performing Fenton's reaction, as oxalate precipitation proved ineffective for U. With organics eliminated from the sample matrices, the samples were diluted to 400 mL with deionized H_2O, and 1 mL of Fe(III) stock solution (2 mg mL^{-1}) was added. The solution was magnetically stirred at 500 rpm, and 30% NH_4OH was added dropwise as necessary to coprecipitate actinides with Fe-hydroxides at pH 7−8. Fe-hydroxides were decanted, centrifuged, and prepared for radiochemical separations.

Radiochemical Separations. The procedures used to sequentially separate Pu, then U, and then Am from samples (once processed as above) are described in detail by Chaplin *et al.*[17] Briefly, solid-phase extraction is used to first isolate Pu

onto Bio-Rad AG 1-X4 resin, then U from the column waste is extracted onto the UTEVA resin, and finally Am from the column waste is extracted onto the IIP-Y^{3+} resin. Certain samples did not require all three separation stages. Pu and then U were sequentially eluted from KMS-1-configured DGT samplers using these steps, while only the Am extraction procedure was required for IIP-Y^{3+}-configured DGT samplers. Likewise, Pu and then Am were separated from the oxalate-precipitated aliquot of seaweed fractions, while only the U extraction procedure was required for the aliquot of seaweed fractions that underwent Fenton's reaction instead of oxalate precipitation. The eluates of all samples were evaporated to dryness and prepared for the manufacture of AMS targets.

AMS Measure. Eluates from radiochemical separations were redissolved in 20 mL of 1 M HCl, and 1 mL of Fe(III) stock solution (2 mg mL^{-1}) was added. The actinides were coprecipitated with Fe-hydroxide at pH 7−8 by dropwise addition of concentrated (30%) NH_4OH. The precipitate was centrifuged, desiccated at 80 °C, and baked at 650 °C for at least 4 h to convert Fe into the oxide form. 2−3 mg of added Nb powder was homogenized with the baked sample powder using a spattle. The powder was compressed into a modified NEC cathode as per ETH Zürich's Laboratory of Ion Beam Physics internal procedure.[20] U measurements were normalized to the in-house ZUTRI standard,[20] and Pu measurements were normalized to the in-house can standard.[20] Am measurements were normalized to a standard produced from certified NIST-traceable [241]Am and [243]Am sources provided by the Radiometrology group of Lausanne University Hospital's Institute of Radiation Physics. Measurements were performed using either the TANDY or MILEA cAMS systems.[20]

Seawater Fraction Calculations. A_c is the concentration of the isotope in the colloidal fraction, calculated according to eq 2

$$A_c = \frac{A_r - A_p}{cf_{UF}} \qquad (2)$$

Here, A_r is the concentration of the isotope in the retentate fraction and A_p is the concentration of the isotope in the permeate fraction. The recovery (R, %) from the ultrafiltration process was calculated according to eq 3

$$R = \frac{A_p + A_c}{A_b} \times 100 \qquad (3)$$

Here, A_b is the concentration of the isotope in the bulk (direct measure) aliquot.

c_{DGT} Calculations. The time-weighted average labile concentration at the interface of the DGT sampler and seawater, c_{DGT}, was derived from the relationship in eq 4

$$\frac{1}{A} = \frac{1}{c_{DGT} \cdot S \cdot t}\left(\frac{\Delta g}{D_M^{gel}} + \frac{\delta^{dbl}}{D_M^w} \right) \qquad (4)$$

where A is the mass of the isotope captured in the binding gel (measured by AMS from the binding gel eluates); Δg is the material diffusive layer (cm) consisting of a 0.014 cm filter membrane plus either a 0.039 cm or 0.078 cm polyacrylamide diffusive gel as used during deployment; D_M^{gel} is the diffusion coefficient (cm^2 s^{-1}) of the metal in the polyacrylamide gel (taken from Table 1 of Chaplin *et al.*[17] as D for commercial aquarium seawater for Pu and Am) or natural seawater-Ravenglass Estuary for U; S is the surface area of the exposed
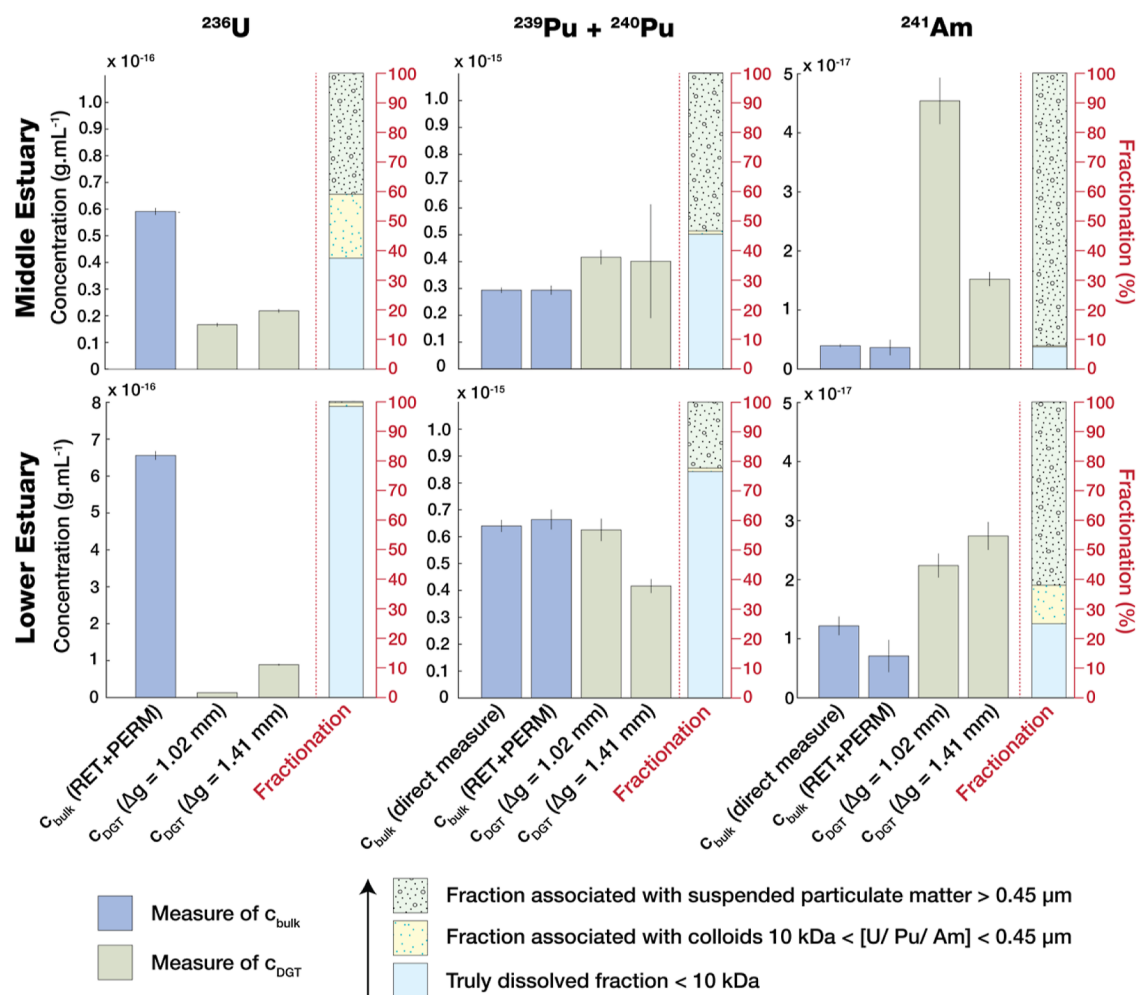
Figure 2. Actinide concentrations according to bulk seawater samples and DGT measures, and association with SPM and colloids. Left to right: c_{bulk} according to direct measure of bulk filtered (0.45 μm) seawater; c_{bulk} according to sum of retentate and permeate ultrafiltered fractions (RET + PERM); c_{DGT} according to DGT sampler with 0.39 mm diffusive gel; c_{DGT} according to DGT sampler with 0.78 mm diffusive gel; (right of dotted red line): distribution of fractions associated with SPM (>0.45 μm), associated with colloids (from 10 kDa to 0.45 μm) and truly dissolved (<10 kDa). $\pm 2\sigma$ type A uncertainties.

filter membrane (cm^2); and t is the deployment time (s). The thickness of the diffusive boundary layer δ^{dbl} (cm) was considered as 0.049 cm for all actinides, as reported by Cusnir *et al.* for Pu[26] and Chaplin et al. for Am.[17] D_M^w is the diffusion coefficient (cm^2 s^{-1}) of the metal in water according to eq 5

$$D_M^w = \frac{D_M^{gel}}{0.85} \tag{5}$$

Uncertainty Calculations. Uncertainty determinations on each mass concentration value were calculated using quadratic propagation of 2σ individual uncertainties on each parameter. Because CF and isotopic ratios are ratios between two mass concentrations, total uncertainty on CF and isotopic ratios was also obtained through a quadratic propagation of uncertainty on each of the concentrations.

RESULTS AND DISCUSSION

Actinide Geochemical Behavior. Our results showed that the increasingly nonconservative (particle reactive) behavior of each target actinide in the order U < Pu < Am[15] was reflected by an increased fraction found associated with SPM at each of the middle and lower estuary sites (Figure 2).

Beginning with U, we focused on tracing the ^{236}U isotope, which is exclusively anthropogenic. c_{DGT} and c_{bulk} both indicated higher ^{236}U concentrations at the lower estuary site than at the middle estuary site. This demonstrates that the input of freshwater from the Esk river (which comes from the Northern Fells of the UK's Lake District and is therefore meteoric with very little ^{236}U content) is more prominent at the middle estuary site. This is reflected in the ^{238}U concentration of the middle estuary water (1.42 $\pm$ 0.02 μg L^{-1}), which is significantly lower than those at the lower estuary site (2.67 $\pm$ 0.04 μg L^{-1}) and the global ocean average (3.3 $\pm$ 0.2 μg L^{-1}).[27] Furthermore, the ^{236}U/^{238}U ratio of the spot-sampled water at the middle estuary site (8.88 $\pm$ 0.14 $\times$ 10^{-8}) indicates less U of anthropogenic origin than the higher ^{236}U/^{238}U ratio at the lower estuary site (2.54 $\pm$ 0.04 $\times$ 10^{-7}). Both of these ratios are higher than the Irish Sea signature further south at Traeth Melynog in January 2019 (5.9 $\pm$ 0.2 $\times$ 10^{-8}).[28] This suggests that a localized input with higher ^{236}U/^{238}U exists in the Esk Estuary; porewater from an adjacent marsh has an elevated ^{236}U/^{238}U ratio of 7.06 $\pm$ 0.01 $\times$ 10^{-7}, and ^{236}U remobilization fluxes from sediments in the Esk Estuary are in the order of 10^{-17}–10^{-15} g h cm^2,[29] suggesting that U remobilization from these and/or surround-
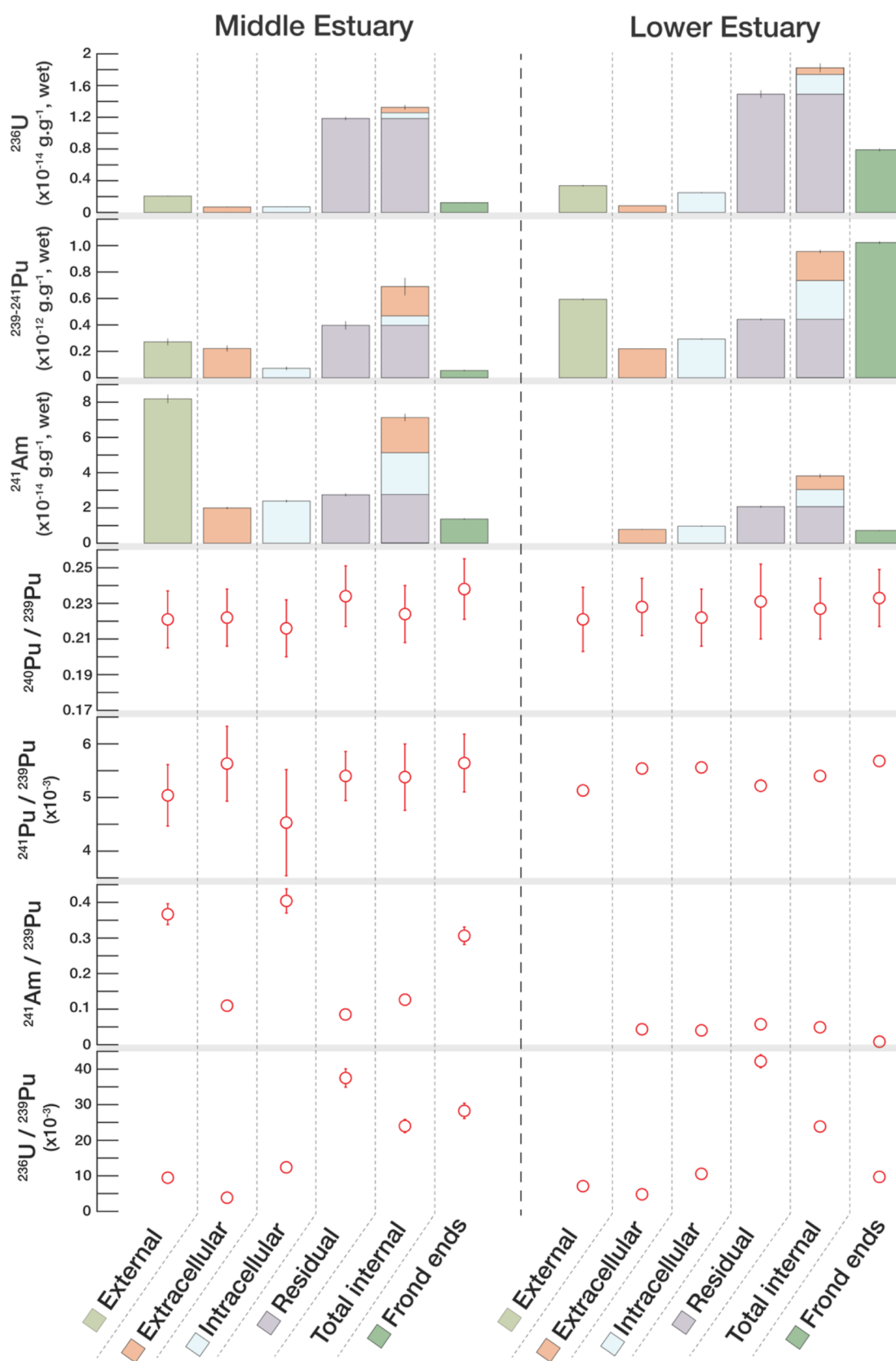
Figure 3. Actinide fractionation and isotopic reports within *F. vesiculosis*. Total concentration, fractionation, and isotopic and elemental signatures (atom/atom) of U, Pu, and Am isotopes in *F. vesiculosis* at middle and lower estuary sites in the Esk Estuary. $^{241}Pu/^{239}Pu$ ratios decay-corrected to 15.01.2021. $\pm 2\sigma$ type A uncertainties.

ing areas has elevated the $^{236}U/^{238}U$ signature of the Esk Estuary waters.

The time-averaged $c_{DGT}(^{236}U)$ was significantly lower than the spot-sampled $c_{bulk}(^{236}U)$ at each site. This effect was more
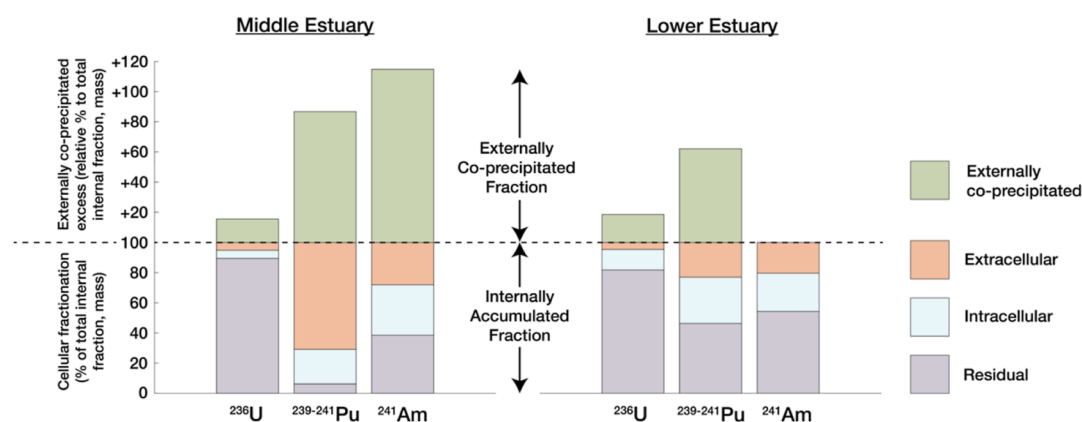
Figure 4. Actinide fractionation within *F. vesiculosis*. Externally and internally accumulated actinide fractions. Internally accumulated fraction distinguished into extracellular, intracellular, and residual fractions.

pronounced at the lower estuary site which is situated closer to the Irish sea ($c_{DGT}/c_{bulk} = 0.078 \pm 0.005$, Figure 2) than that at the middle estuary site ($c_{DGT}/c_{bulk} = 0.33 \pm 0.02$, Figure 2). Because U is conservative and mostly present in seawater as opposed to associated with sediments (as is especially the case in the lower estuary Figure 1), spot sampling might significantly overestimate the time-averaged U concentration at high tide where significant fluctuations in the seawater constituent occur over the tidal cycle. We previously demonstrated in a laboratory context that $c_{DGT}(U) = c_{bulk}(U)$ using the KMS-1 DGT configuration in water taken from the lower estuary site,[17] where U behaves in a highly conservative fashion by occurring almost exclusively in the truly dissolved phase (Figure 2). This indicates that any differences observed in $c_{DGT}(^{236}U)$ and $c_{bulk}(^{236}U)$ are due to the dynamic hydraulic regime, underlining that $c_{bulk}(^{236}U)$ was not representative throughout the deployment period. As a result, we consider that it is more valid to use a time-integrated sampling method to better represent the overall U concentration to which the biota is exposed. This is particularly applicable to estuary systems such as the Esk Estuary, where a macrotidal regime drives continuous and significant physicochemical fluctuations.[19]

c_{DGT} and c_{bulk} demonstrated that the $^{239}Pu + ^{240}Pu$ concentrations at the lower estuary were approximately twice the concentrations at the middle estuary, whereas the ^{236}U concentration was also elevated at the lower estuary but by a factor of 10 (Figure 2). This indicates that Pu possibly behaved somewhat more conservatively than can be expected from its k_d; the truly dissolved fraction accounted for $77 \pm 6\%$ of total Pu in the lower estuary and in the middle estuary. Furthermore, c_{DGT} and c_{bulk} were closely replicated for Pu at both sampling locations. c_{DGT} has been demonstrated to closely reproduce the solution concentrations of Pu(IV) and Pu(V) when using the same diffusion coefficient derived for Pu(IV + V) at equilibrium in seawater,[17] indicating that Pu(IV) and Pu(V) can be treated as a single DGT analyte in marine waters without knowledge of the oxidation state. The advantage of this was demonstrated at the middle estuary site, where less Pu was found associated with SPM ($45.3 \pm 3.3\%$) than in the lower estuary, possibly indicating a larger fraction of particle-reactive Pu(IV), but there was nonetheless a close correspondence between c_{DGT} and c_{bulk} as observed in the lower estuary (Figure 1). Additionally, we found the colloid-associated Pu fraction to be very little in seawater at either the

lower ($1.2 \pm 0.1\%$) or middle ($1 \pm 0.1\%$) Esk Estuary (Figure 2). This aligns with previous work with north-eastern Irish Sea water, which found no significant enrichment of A_r (see methods) for Pu across a range of ultrafilters (10, 3, 1 kDa),[1] concluding that little, if any, Pu was colloid-associated. We tentatively attribute the consistency of these findings to the carbonate content of seawater forming carbonate-supported plutonyl complexes, for example, $[Pu(V)O_2(CO_3)_n]^{m-}_{(aq)}$ and/or Pu-dioxide $[Pu(IV)O_2(CO_3)_n]^{m-}$ species, which are possibly fully labile with no significant effect of [Pu]-ligand dissociation.

Americium was observed to be mostly associated with SPM at both sampling sites, which is logical given its very high sediment-water k_d.[15] Additionally, $13.0 \pm 5.1\%$ of Am was colloid-associated in the lower estuary, which could demonstrate that [Am]-colloid complexes in seawater may dissociate due to Am^{3+} having a higher affinity for SPM such as sediment particles. In the middle estuary, the DGT sampler with the thinner diffusive gel ($\Delta g = 1.02$ cm) provided a significantly higher calculation of c_{DGT} than the DGT sampler with $\Delta g = 1.41$ cm. This possibly indicates that [Am]-ligand complexes have a low lability; this is not observed in the lower estuary, where the input of organic material in the sandy channel would not be as high as at the middle estuary site adjacent to the saltmarsh. The additional input of SPM and organic matter from the saltmarsh is indicated by the proportion of U, Pu, and Am associated with SPM being higher at the middle estuary site than at the lower estuary in every instance (Figure 2). Taking a comparison between c_{DGT} at each site calculated by the DGT sampler of $\Delta g = 1.02$ cm, c_{DGT} was around twice as high in the middle estuary compared to the lower estuary, while the opposite was observed for c_{bulk}. This most likely reflects an additional flux of Am from the adjacent saltmarsh in the middle estuary; this would not be considered by c_{bulk} of our spot-sampled water at the point of high tide before the saltmarsh has been inundated for some time, but this would however be integrated into the time-averaged c_{DGT}. This further illustrates how the DGT technique is more suited to dynamic estuary systems than a time- and site-specific sample. We additionally detected ^{244}Cm in some of the IIP-Y^{3+} DGT resin-gel eluates used to monitor Am, with only a few counts around the detection limit of the AMS. As the IIP-Y^{3+} DGT resin gel has been shown to capture Cm,[29] future environmental analysis of Cm using DGT could therefore be feasible, particularly at a more contaminated site.

Regarding the target actinides as a whole, in 2015, Daneshvar reported that Fe concentrations in Ravenglass Estuary water samples decrease rapidly as salinity increases, with low Fe concentrations in samples once salinity exceeds 5000 mg L^{-1} (presumably due to flocculation of colloidal Fe-oxides, Fe-hydroxides, and Fe-organic complexes).[19] This results in the precipitation of a large proportion of incoming Fe. Actinides are known to coprecipitate with Fe-hydroxides, thus, actinide concentrations will be strongly influenced in the Ravenglass Estuary by freshwater and seawater mixing. As a result, we consider that the use of a time-weighted average sampling technique would better reflect the overall concentration of the actinides in the water to which the biota is exposed over time with tidal cycles.

Implications for Actinide Bioaccumulation and Fractionation. To investigate the effect of SPM and/or colloid-association on bioaccumulation and internal fractionation, SE was performed on *F. vesiculosis* samples retrieved adjacent to the sites of DGT deployment in the middle and lower estuary (Figures 3 and 4). As with the SPM-associated fraction in seawater, the fraction of each actinide externally coprecipitated on the fronds increased in the order of its particle reactivity (U < Pu < Am). The largest proportion of U was found in the residual fraction of the seaweeds at both the middle estuary and lower estuary sites (Figures 3 and 4). As with U, Pu was also found mostly internally but with a more significant fraction externally precipitated on the fronds than U. Internal Pu was however more evenly distributed throughout *F. vesiculosis* between the extracellular, intracellular, and residual fractions, rather than concentrated in the residual fraction as with U. Am was mostly found externally accumulated on the fronds, reflecting its high particle reactivity and consequent association with physisorbed SPM or coprecipitation with CaCO$_3$. These observations indicate that conservative U and Pu to a lesser extent are more preferentially incorporated inside *F. vesiculosis* and metabolized, for example, *via* the pathway [root/surface diffusion > phloem > cell surface > cytosol]. Conversely, particle-reactive Am is preferentially deposited externally, while a significant fraction can nonetheless become internally incorporated and metabolized throughout different internal compartments once transferred to the phloem.

Neither environmental fractionation nor biofractionation significantly alters $^{240}Pu/^{239}Pu$ and $^{241}Pu/^{239}Pu$ ratios due to the high AMU of Pu isotopes and the fact that the isotopes are of the same element. In this sense, variations will not be significant between the *F. vesiculosis* fractions, but the $^{240}Pu/^{239}Pu$ and $^{241}Pu/^{239}Pu$ signatures can rather indicate the source of the Pu. The $^{240}Pu/^{239}Pu$ and $^{241}Pu/^{239}Pu$ signatures of the *F. vesiculosis* fractions are all significantly above global fallout ratios (Figure 3), reflecting further work which indicates that biota in this estuary have accumulated sediment-remobilized Pu.[29] By analyzing the atomic ratios between anthropogenic isotopes of different radioelements ($^{236}U/^{239}Pu$, $^{241}Am/^{239}Pu$), elemental fractionation as a function of the biogeochemistry of the actinide and its biological metabolism by *F. vesiculosis* can be assessed. The $^{236}U/^{239}Pu$ ratio is significantly elevated in the residual fraction over all others, demonstrating that U is mostly biologically mobile and traverses the entire [root/surface diffusion > phloem > cell surface > cytosol] pathway, resulting in the majority fraction becoming strongly bound intracellularly. It is also worth considering that the oxidation state of some metals

may change upon association with an organism or particle, rendering those metals much less available for release.[15] In this case, there is possibly a reducing effect within the cytosol which could have altered labile [U(VI)]-species to more particle-reactive [U(IV)].

The $^{241}Am/^{239}Pu$ signatures of the middle estuary *F. vesiculosis* fractions are higher than the lower estuary *F. vesiculosis* fractions, indicating that a higher % association with SPM leads to preferential external deposition of Am likely due to a higher influence of physisorption of SPM-associated Am to the *F. vesiculosis* fronds. Due to Am's high particle reactivity, the $^{241}Am/^{239}Pu$ signature strongly decreases from the external to extracellular fraction, which is particularly evidenced in the lower estuary. The *F. vesiculosis* frond tips (outmost <2.5 cm of the thallus) were generally much less contaminated than the bulk plant, representing newer seasonal growth. Given standard sampling methods for the bulk biota samples, the sum of all four *F. vesiculosis* fractions was considered when calculating the CFs (Figure 5).
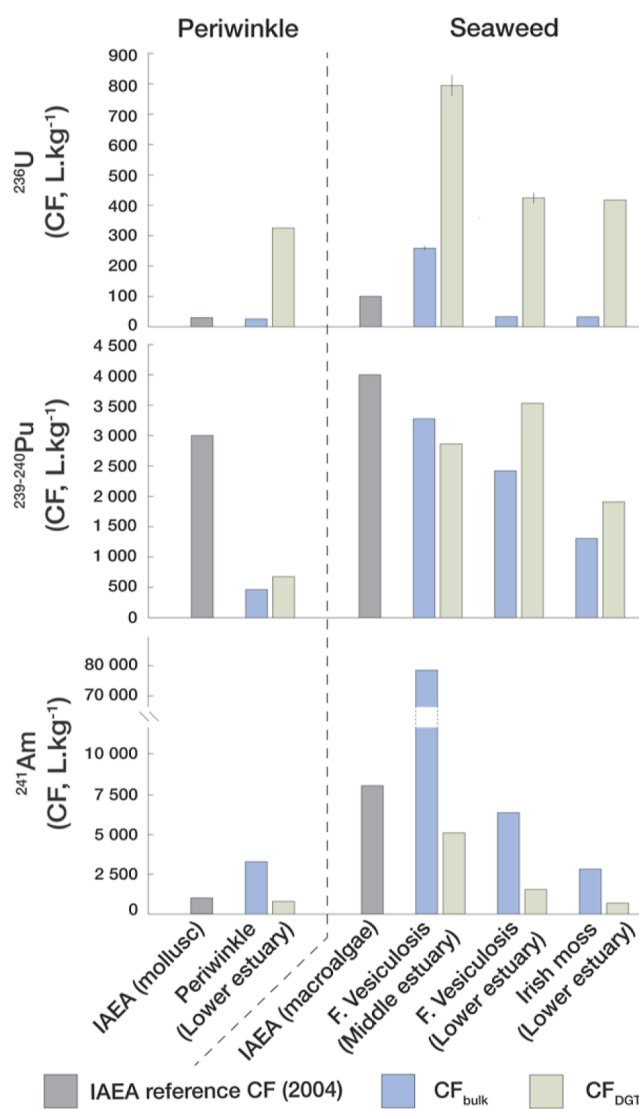

Figure 5. Comparison of CFs from DGT measures, bulk measures, and IAEA reference CFs. Note: error bars are not visible in every case at the scale of the figure.

Implications for Actinide CFs. Figure 5 compares the IAEA reference CFs for molluscs and macroalgae with those calculated in this work for *Littorina littorae* (*L. littorae*), *F. vesiculosis*, and *Chondrus crispus* (*C. crispus*) using both c_{DGT} (CF_{DGT}) and a single spot sample retrieved at the middle estuary site (high tide) and the lower estuary site (low tide), c_{bulk} (CF_{bulk}). $CF_{bulk}(^{236}U)$ in *L. littorae*, *F. vesiculosis,* and *C. crispus* is closer to the respective mollusc and macroalgae IAEA reference values. However, $CF_{DGT}(^{236}U)$ is significantly higher, which additionally reflects a strong internalization of U as observed with the preferential accumulation of ^{236}U in the residual *F. vesiculosis* SE fractions. In this sense, the spot sample used to calculate $CF_{bulk}(^{236}U)$, taken at its specific time and date, does not agree with the time-integrated $CF_{DGT}(^{236}U)$ and significantly underestimates the CF for ^{236}U in each species.

$CF_{DGT}(^{239+240}Pu)$ and $CF_{bulk}(^{239+240}Pu)$ for *F. vesiculosis* were more closely comparable for Pu and close to the IAEA reference values. This possibly indicates Pu is less particle-reactive than otherwise thought and described in the literature; similar work with Pu and DGT in a karstic freshwater system also demonstrated that Pu is mobile and fully bioavailable.[25] $CF_{DGT}(^{239+240}Pu)$ and $CF_{bulk}(^{239+240}Pu)$ were also comparable for *L. littorae* but both significantly below the IAEA reference value for molluscs. It must also be considered that phylogenetic effects may affect the CF in an organism and may possibly be more specific at the species or even subspecies level, demonstrating further scope to define more accurate CFs.

$CF_{bulk}(^{241}Am)$ overestimates the CF in *L. littorae* and *F. vesiculosis* compared to the specific spot sample used to calculate $CF_{DGT}(^{241}Am)$. As mentioned in previous sections, CF_{DGT} is particularly applicable in the Esk estuary where extreme temporal fluctuations in $CF_{bulk}(^{241}Am)$ can be expected as a function of varying inputs of ^{241}Am-enriched seawater and ^{241}Am-depleted meteoritic freshwaters and the remobilization of particulate-associated ^{241}Am, and this is most probably the reason for this difference.

Overall Implications of the Study. Our results demonstrated a constant reproducible trend in the behavior of anthropogenic actinides in the Esk estuary, from seawater concentrations to incorporation within the biota. An important implication of the complicated hydrological regime in the Esk estuary lies in the difference between c_{bulk} and c_{DGT} observed for conservative (U) and particle-reactive (Am) species, which has implications for the determination of CFs. Therefore, we propose that time-integrated sampling, as can be undertaken by DGT, can provide an important tool to better constrain and represent the overall actinide concentration to which aquatic biota are exposed over time. This is particularly pertinent for estuary systems, and especially for macrotidal systems such as the Esk Estuary, which have a high range of salinity, pH, and ion content throughout the tidal cycle. We observe that U is significantly present in Esk Estuary seawater as a conservative radionuclide, while Am is much more sensitive to the influence of tidal movement as a nonconservative radionuclide which is only present in negligible quantities in meteoric waters. Overall, the increasing particle reactivity gradient in the order of [U < Pu < Am] has a strong influence on SPM association and internalization within *F. vesiculosis*, which is demonstrated by the elemental fractionation between the *F. vesiculosis* SE fractions. We note that traditional CF calculation which uses spot-sampled bulk water and/or the IAEA reference value significantly underestimated the bioaccumulation of U in both a mollusc and two species of seaweed compared to time-integrated DGT sampling. Differences were not significant for Pu, but spot sampling significantly overestimated the CFs for Am. We therefore recommend that further studies are carried out with DGT to investigate our hypothesis. With increased datasets using the DGT technique, a robust case for the revision of CFs may well be able to be built. In this case, CFs may potentially show less dispersion if calculated by using a time-integrated bioavailability proxy such as DGT instead of specific spot-sampled bulk water.

■ AUTHOR INFORMATION

Corresponding Authors

Joshua D. Chaplin − *Institute of Radiation Physics, Lausanne University Hospital and University of Lausanne, Lausanne 1007, Switzerland;* ⓞ orcid.org/0000-0002-6151-1942; Email: joshua.chaplin@chuv.ch

Pascal Froidevaux − *Institute of Radiation Physics, Lausanne University Hospital and University of Lausanne, Lausanne 1007, Switzerland;* ⓞ orcid.org/0000-0003-0077-0294; Email: pascal.froidevaux@chuv.ch

Authors

Marcus Christl − *Laboratory of Ion Beam Physics, ETH Zürich, Zürich 8093, Switzerland;* ⓞ orcid.org/0000-0002-3131-6652

Andrew B. Cundy − *School of Ocean and Earth Science, University of Southampton, National Oceanography Centre, European Way, Southampton SO14 3ZH, U.K.;* ⓞ orcid.org/0000-0003-4368-2569

Phillip E. Warwick − *School of Ocean and Earth Science, University of Southampton, National Oceanography Centre, European Way, Southampton SO14 3ZH, U.K.*

Paweł Gaca − *School of Ocean and Earth Science, University of Southampton, National Oceanography Centre, European Way, Southampton SO14 3ZH, U.K.*

François Bochud − *Institute of Radiation Physics, Lausanne University Hospital and University of Lausanne, Lausanne 1007, Switzerland*

Complete contact information is available at:
https://pubs.acs.org/10.1021/acsestwater.2c00194

Author Contributions

field deployments, interpreted experimental data, and contributed to the manuscript.

Notes

The authors declare no competing financial interest.

■ REFERENCES

(1) Mitchell, P. I.; Downes, A. B.; Vintró, L. L.; McMahon, C. A. Studies of the speciation, colloidal association and remobilisation of plutonium in the marine environment. *Radioact. Environ.* 2001, 1, 175−200.

(2) Howard, B. J.; et al. The IAEA handbook on radionuclide transfer to wildlife. *J. Environ. Radioact.* 2013, 121, 55−74.

(3) Carroll, J.; Harms, I. H. Uncertainty analysis of partition coefficients in a radionuclide transport model. *Water Res.* 1999, 33, 2617−2626.

(4) Fisher, N. S.; et al. Radionuclide bioconcentration factors and sediment partition coefficients in Arctic Seas subject to contamination from dumped nuclear wastes. *Environ. Sci. Technol.* 1999, 33, 1979−1982.

(5) Gil-García, C.; Tagami, K.; Uchida, S.; Rigol, A.; Vidal, M. New best estimates for radionuclide solid-liquid distribution coefficients in soils. Part 3: Miscellany of radionuclides (Cd, Co, Ni, Zn, I, Se, Sb, Pu, Am, and others). *J. Environ. Radioact.* 2009, 100, 704−715.

(6) McDonald, P.; Vives i Batlle, J. V.; Bousher, A.; Whittall, A.; Chambers, N. The availability of plutonium and americium in Irish Sea sediments for re-dissolution. *Sci. Total Environ.* 2001, 267, 109−123.

(7) Swift, D. J.; Nicholson, M. D. Variability in the edible fraction content of 60Co, 99Tc, 110mAg, 137Cs and 241Am between individual crabs and lobsters from Sellafield (north eastern Irish Sea). *J. Environ. Radioact.* 2001, 54, 311−326.

(8) Tagami, K.; Uchida, S. Marine and freshwater concentration ratios (CRwo-water): Review of Japanese data. *J. Environ. Radioact.* 2013, 126, 420−426.

(9) Warwick, P. E.; Cundy, A. B.; Croudace, I. W.; Bains, M. E. D.; Dale, A. A. The uptake of iron-55 by marine sediment, macroalgae, and biota following discharge from a nuclear power station. *Environ. Sci. Technol.* 2001, 35, 2171−2177.

(10) Morris, K.; Butterworth, J. C.; Livens, F. R. Evidence for the remobilization of Sellafield waste radionuclides in an intertidal salt marsh, West Cumbria, U.K. *Estuar. Coast Shelf Sci.* 2000, 51, 613.

(11) Hunt, J.; Leonard, K.; Hughes, L. Artificial radionuclides in the Irish Sea from Sellafield: Remobilisation revisited. *J. Radiol. Prot.* 2013, 33, 261.

(12) Kershaw, P.; Pentreath, R. J.; WoodheadHunt, D. S. G. J. A review of radioactivity in the Irish Sea. *Aquat. Environ. Monit. Rep.* 1992, 32.

(13) Aldridge, J. N.; et al. Transport of plutonium (239/240Pu) and caesium (137Cs) in the Irish Sea: Comparison between observations and results from sediment and contaminant transport modelling. *Continent. Shelf Res.* 2003, 23, 869−899.

(14) Chaplin, J. D.; et al. Effective 137Cs+ and 90Sr2+ immobilisation from groundwater by inorganic polymer resin Clevasol embedded within a macroporous cryogel host matrix. *Mater. Today Sustainability* 2022, 19, 100190.

(15) International Atomic Energy Agency. Sediment Distribution Coefficients and Concentration Factors for Biota in the Marine Environment. *Technical Reports Series No.422*, 2004.

(16) Davison, W.; Zhang, H. In situ speciation measurements of trace components in natural waters using thin-film gels. *Nature* 1994, 367, 546−548.

(17) Chaplin, J. D.; Warwick, P. E.; Cundy, A. B.; Bochud, F.; Froidevaux, P. Novel DGT Configurations for the Assessment of Bioavailable Plutonium, Americium, and Uranium in Marine and Freshwater Environments. *Anal. Chem.* 2021, 93, 11937−11945.

(18) Chaplin, J. D.; Christl, M.; Straub, M.; Bochud, F.; Froidevaux, P. Passive Sampling Tool for Actinides in Spent Nuclear Fuel Pools. *ACS Omega* 2022, 7, 20053.

(19) Daneshvar, E. Dissolved Iron Behavior in the Ravenglass Estuary Waters, An Implication on the Early Diagenesis. *Univers. J. Geosci.* 2015, 3, 1.

(20) Christl, M.; et al. The ETH Zurich AMS facilities: Performance parameters and reference materials. *Nucl. Instrum. Methods Phys. Res. Sect. B Beam Interact. Mater. Atoms* 2013, 294, 29−38.

(21) Manos, M. J.; Kanatzidis, M. G. Highly efficient and rapid Cs + uptake by the layered metal sulfide K 2xMn xSn 3-xS 6 (KMS-1). *J. Am. Chem. Soc.* 2009, 131, 6599−6607.

(22) Chauvin, A. S.; Bünzli, J. C. G.; Bochud, F.; Scopelliti, R.; Froidevaux, P. Use of dipicolinate-based complexes for producing ion-imprinted polystyrene resins for the extraction of yttrium-90 and heavy lanthanide cations. *Chem.—Eur. J.* 2006, 12, 6852−6864.

(23) Cusnir, R.; Steinmann, P.; Christl, M.; Bochud, F.; Froidevaux, P. Speciation and Bioavailability Measurements of Environmental Plutonium Using Diffusion in Thin Films. *JoVE* 2015, 105, e53188.

(24) Vázquez, M. D.; López, J.; Carballeira, A. Modification of the sequential elution technique for the extraction of heavy metals from bryophytes. *Sci. Total Environ.* 1999, 241, 53.

(25) Cusnir, R.; Christl, M.; Steinmann, P.; Bochud, F.; Froidevaux, P. Evidence of plutonium bioavailability in pristine freshwaters of a karst system of the Swiss Jura Mountains. *Geochim. Cosmochim. Acta* 2017, 206, 30−39.

(26) Cusnir, R.; et al. Probing the Kinetic Parameters of Plutonium-Naturally Occurring Organic Matter Interactions in Freshwaters Using the Diffusive Gradients in Thin Films Technique. *Environ. Sci. Technol.* 2016, 50, 5103−5110.

(27) Ku, T. L.; Knauss, K. G.; Mathieu, G. G. Uranium in open ocean: concentration and isotopic composition. *Deep Sea Res.* 1977, 24, 1005.

(28) Castrillejo, M.; et al. Unravelling 5 decades of anthropogenic 236U discharge from nuclear reprocessing plants. *Sci. Total Environ.* 2020, 717, 137094.

(29) Chaplin, J. D.; et al. Bioavailable actinide fluxes to the Irish Sea from Sellafield-labelled sediments. *Water Res.* 2022, 221, 118838.